

# ASSESSMENT OF RIGHT VENTRICULAR STRUCTURE AND FUNCTION IN PULMONARY HYPERTENSION

JULIA GRAPSA, MD, DAVID DAWSON, MSc AND  
PETROS NIHOYANNOPOULOS, MD, FRCP, FACC, FESC

DEPARTMENT OF CARDIOVASCULAR SCIENCES, IMPERIAL COLLEGE OF LONDON, NATIONAL HEART AND LUNG INSTITUTE, HAMMERSMITH HOSPITAL, LONDON, UK

Right ventricular function plays an important role in determining cardiac symptoms and exercise capacity in chronic heart failure. It is known that right ventricle has complex anatomy and physiology. The purpose of this review paper is to demonstrate the best assessment of the right ventricle with current echocardiography. Echocardiography can assess sufficiently right ventricular structure and function and also suggest prognosis in pulmonary hypertension patients, especially with the use of modern imaging techniques. Finally, the new imaging modality of real time three dimensional echocardiography is interchangeable to cardiac magnetic resonance in reproducibility and accuracy.

**KEY WORDS:** Right ventricle · Echocardiography · Cardiac magnetic resonance.

## INTRODUCTION

Right ventricular (RV) function plays an important role in determining cardiac symptoms and exercise capacity in chronic heart failure. The purpose of this review paper is to demonstrate the best assessment of the RV with current echocardiography.

## RIGHT VENTRICULAR ANATOMY

The complex anatomy of the RV is an important consideration in its assessment.<sup>1)</sup> It is the most anteriorly situated cardiac chamber, located immediately behind the sternum.<sup>1)</sup> It also marks the inferior border of the cardiac silhouette. In contrast to the near conical shape of the left ventricle (LV), the RV is more triangular in shape when viewed from the front and it curves over the LV. In cross section the normal cavity appears crescentic. Thus, the curvature of the ventricular septum places the RV outflow tract antero-cephalad to that of the LV resulting in a characteristic “cross-over” relationship between right and LV outflows. Two anatomical components which make the RV difficult to examine in detail, especially when using two-dimensional echocardiography, are the irregular shape of the cavity and the heavy trabeculation making the identification of RV borders difficult.<sup>1,3)</sup>

## TWO DIMENSIONAL ECHOCARDIOGRAPHY

The protocol of the views required for two dimensional echocardiography is demonstrated at Table 1. The comparison of findings in healthy people compared to patients with pulmonary hypertension (PH) is demonstrated in Table 2.

## PARASTERNAL LONG AXIS VIEW OF THE LEFT VENTRICLE

The anterior wall of the RV is seen immediately behind the chest wall. The RV outflow tract appears as a triangular echo-free structure about 1/3 of the size of the more posterior LV. During systole, the anterior wall of the RV thickens and the RV cavity becomes smaller as the ventricle contracts.<sup>1-3)</sup> However in PH when the RV is pressure loaded, the RV is more prominent with the free wall hypertrophied and globally hypokinetic.

## PARASTERNAL LONG AXIS VIEW OF RIGHT VENTRICULAR INFLOW TRACT

In PH, the RV apex is hypertrophied and the cavity is dilated. The assessment of RV systolic function is best performed in this view. The papillary muscles of the RV are usually hypertrophied and they are easily distinguished. Typically, there

• Received: August 3, 2011 • Revised: August 12, 2011 • Accepted: August 17, 2011

• Address for Correspondence: Petros Nihoyannopoulos, Department of Cardiovascular Sciences, Imperial College of London, National Heart and Lung Institute, Hammersmith Hospital, Du Cane Road, London W12 0NN, UK Tel: +44-208-383-3948, Fax: +44-208-383-4392, E-mail: p.nihoyannopoulos@imperial.ac.uk

• This is an Open Access article distributed under the terms of the Creative Commons Attribution Non-Commercial License (<http://creativecommons.org/licenses/by-nc/3.0>) which permits unrestricted non-commercial use, distribution, and reproduction in any medium, provided the original work is properly cited.

are two principal papillary muscles (anterior and posterior) with a smaller suprasternal (or conus) papillary muscle. In this view the tricuspid annulus can be imaged and its diameter measured. The normal range is between 1.3 and 2.8 cm in systole.<sup>1-3)</sup> Two of the three tricuspid valve leaflets are seen: the anterior and septal leaflets.<sup>2)</sup> Assessment of tricuspid leaflet mobility and systolic apposition is important for the exclusion of any primary cause of tricuspid valve disease such as rheumatic fever (with involvement of mitral valve in most of the cases),

carcinoid, sarcoidosis or endocarditis. In secondary tricuspid insufficiency due to RV dilatation, the leaflets are normal with reduced apposition secondary to tricuspid annular dilatation.<sup>2)</sup>

**PARASTERNAL LONG AXIS VIEW OF THE RIGHT VENTRICULAR OUTFLOW TRACT**

The normal RV outflow tract dimension is 1.8-3.4 cm in diastole.<sup>1-3)</sup> The determination of the dilatation of pulmonary artery is important for the diagnosis of PH. The normal diam-

**Table 1.** Protocol of two dimensional echocardiography

<p>Parasternal window</p> <ul style="list-style-type: none"> <li>· Parasternal long-axis of the left ventricle</li> <li>· Parasternal long-axis of the right ventricular inflow/outflow tract</li> <li>· Parasternal short-axis of the left ventricle (aortic root level, mitral valve level, papillary muscles, apical view)</li> </ul> <p>Apical window</p> <ul style="list-style-type: none"> <li>· Apical “four-chamber” view (including both atrio-ventricular valves)</li> <li>· Apical “five-chamber” view (including left ventricular outflow tract)</li> </ul> <p>Doppler examination</p> <ul style="list-style-type: none"> <li>· Colour Doppler in all apical projections</li> <li>· Colour Doppler in parasternal projections (long/short axis)</li> <li>· Pulsed-wave Doppler for transmitral velocities</li> <li>· Pulsed-wave Doppler for left ventricular outflow tract</li> <li>· Pulsed-wave Doppler for the tricuspid inflow</li> </ul>	<p>Doppler examination</p> <ul style="list-style-type: none"> <li>· Pulsed-wave Doppler for the right ventricular outflow tract</li> <li>· Continuous-wave Doppler across the left ventricular outflow-aortic valve</li> <li>· Continuous-wave Doppler across the tricuspid valve (for tricuspid regurgitation)</li> <li>· Continuous-wave Doppler across the pulmonary valve (for pulmonary regurgitation)</li> <li>· Tissue Doppler Index of the right ventricular free wall</li> <li>· Tricuspid annular plane systolic exertion (M-mode)</li> </ul> <p>Subcostal view</p> <ul style="list-style-type: none"> <li>· Four-chamber view</li> <li>· Atrial septum</li> <li>· Inferior vena cava</li> </ul>
--	--

**Table 2.** Comparison of findings between healthy and patients with pulmonary hypertension

Echocardiographic views - Two dimensional views	Normal findings	Findings in pulmonary hypertension
Parasternal long axis view of the left ventricle	<ul style="list-style-type: none"> <li>· Right ventricle is &lt; 1/3 of the size of the left ventricle</li> <li>· No evidence of septal bouncing</li> <li>· No evidence of hypertrophy</li> <li>· Left ventricle has normal size</li> </ul>	<ul style="list-style-type: none"> <li>· Dilated and hypertrophied right ventricle</li> <li>· Prominent moderator band</li> <li>· Left ventricle is less than the size of the right ventricle</li> <li>· Deviation of the septum towards the left ventricle</li> </ul>
Parasternal long axis view of right ventricular inflow tract	<ul style="list-style-type: none"> <li>· Good apposition of the tricuspid leaflets with trivial or mild tricuspid regurgitation</li> <li>· Normal size of the right ventricle and atrium</li> </ul>	<ul style="list-style-type: none"> <li>· Dilatation of the right ventricle and atrium</li> <li>· Functional dilatation of the tricuspid annulus and tricuspid regurgitation</li> </ul>
Parasternal long and short axis views of the right ventricular outflow tract	<ul style="list-style-type: none"> <li>· Main pulmonary artery and branches are thin-walled structures and at most there is trivial pulmonary regurgitation</li> </ul>	<ul style="list-style-type: none"> <li>· Dilated pulmonary artery and branches</li> </ul>
Parasternal short axis view of aorta and left atrium	<ul style="list-style-type: none"> <li>· Normal right ventricle, pulmonary artery and branches and tricuspid valve</li> <li>· Intact interatrial septum</li> </ul>	<ul style="list-style-type: none"> <li>· Right ventricular dilatation and hypertrophy, as well as dilatation of the pulmonary artery</li> <li>· Possibility of interatrial septal defect</li> </ul>
Parasternal short axis view as the level of left ventricular papillary muscles	<ul style="list-style-type: none"> <li>· Shape of the left ventricle: circular - eccentricity index equal to 1 both in diastole and systole</li> <li>· Normal size of the right and left ventricles</li> </ul>	<ul style="list-style-type: none"> <li>· D-shaped left ventricle - eccentricity index greater than 1, in systole ± diastole</li> <li>· Dilated and hypertrophied right ventricle</li> <li>· Left ventricle smaller than right ventricle</li> </ul>
Apical four-chamber view	<ul style="list-style-type: none"> <li>· Right ventricle: triangular in shape and less than 1/3 of the size of the left ventricle</li> <li>· The right ventricular apex is nearer the base of the heart than that of the left ventricle</li> <li>· Interventricular and interatrial septum intact</li> </ul>	<ul style="list-style-type: none"> <li>· Pressure and volume loaded right ventricle</li> <li>· Dilated right ventricle and atrium</li> <li>· Hypertrophy</li> <li>· Deviation of the septum towards the left ventricle</li> <li>· Dilated tricuspid annulus</li> <li>· Possibility of interventricular/interatrial septal defect</li> </ul>
Subcostal view	<ul style="list-style-type: none"> <li>· Inferior vena cava normal (1.2-2.3 cm)</li> <li>· Respiratory collapse &gt; 50%</li> </ul>	<ul style="list-style-type: none"> <li>· Dilated inferior vena cava (&gt; 2.3 cm)</li> <li>· Reduced or no respiratory collapse</li> </ul>

eter of main pulmonary artery is 0.9-2.9 cm (corrected to height) and normal annulus diameter is 1-2.2 cm.<sup>1-3)</sup>

#### SHORT AXIS AT THE LEVEL OF LEFT VENTRICULAR PAPILLARY MUSCLES

The RV in PH is often dilated and hypertrophied, such that it compresses the LV, giving it a characteristic D-shaped appearance in systole.

Normally, the LV appears circular in shape, both in systole and diastole. When the RV is pressure-loaded, the ventricular septum deforms and may even curve towards the LV cavity. This distortion may be quantified by the LV eccentricity index which is described later.

#### APICAL FOUR-CHAMBER VIEW

Normally, the RV appears triangular in shape and about the one-third the size of the LV. The apex of the RV is located closer to the base of the heart than that of the LV. However, in PH, the cavity is dilated and hypertrophied to an extent depending on the degree of pressure and volume loading (Fig. 1). The normal wall thickness for the RV (measured at the lateral free wall) is 0.2-0.5 cm ( $0.2 \pm 0.05$  cm/m<sup>2</sup> indexed to body surface area).<sup>1-3)</sup>

When measuring the area of the RV and the right atrium, normal values are as following:<sup>1-3)</sup> RV end-diastole  $20.1 \pm 4$  cm<sup>2</sup>, RV end-systole<sup>1-3)</sup>  $10.9 \pm 2.9$  cm<sup>2</sup> and right atrium in end-systole  $13.5 \pm 2$  cm<sup>2</sup>.

In pulmonary hypertensive patients, RV free wall is the first to become hypertrophied (in parallel with the apex), demonstrate systolic dysfunction and lower tissue myocardial velocities. Modalities such as tissue Doppler imaging, which measure these velocities tend to predict systolic and diastolic dysfunction of the RV free wall.<sup>4-6)</sup> The apex is frequently hypertrophied and akinetic. Careful examination of the RV apex, using zoom and focus modalities, should be performed, to ex-

clude a thrombus or an apical mass.

The hypertrophic moderator band often is seen traversing the RV near the apex.<sup>1)7)8)</sup> Considerable individual variability in the shape and wall motion of the RV, particularly at the apex, is seen in healthy individuals, so caution is needed in diagnosing an abnormal RV from any single tomographic view.

#### SUBCOSTAL VIEW

The subcostal view allows the assessment of RV dysfunction and thickness of RV walls, in patients with difficult parasternal or apical windows. By rotating the transducer inferiorly from the subcostal four-chamber view, a long-axis of the inferior vena cava is obtained as it enters the right atrium. The size of the proximal 2-3 cm of the inferior vena cava at rest and changes in size with respiration are used to estimate right atrial pressure. The hepatic veins (especially the central hepatic vein) are helpful in assessing right atrial pressure and for recording right atrial Doppler filling patterns.<sup>3)</sup> The proximal abdominal aorta is imaged in long axis medial to the inferior vena cava.

#### RIGHT VENTRICULAR PRESSURE VERSUS VOLUME-LOADING

RV volume overload, results from an atrial septal defect, partial abnormal pulmonary venous drainage, tricuspid or pulmonary insufficiency, causes an increase in RV end-systolic and end-diastolic volumes with normal RV ejection fraction.<sup>1-3)</sup> In RV pressure overload the RV dilates with the ventricular septum “pushing” to the left during systole.<sup>4)5)7)8)</sup> An inverse relationship between RV ejection fraction and afterload develops (pulmonary artery pressure or pulmonary vascular resistance). RV pressure overload distorts both LV systolic and diastolic geometry due to the interventricular dependence (Fig. 2).<sup>4)5)</sup> Chronic RV pressure overload causes distortion of the geometrical shape and LV physiology resulting in signifi-

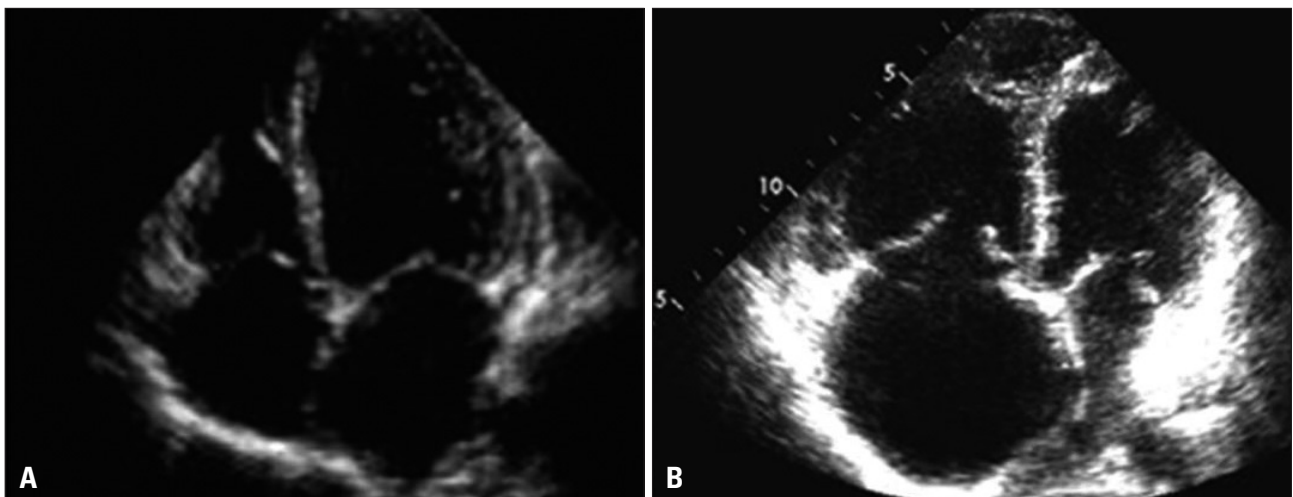


**Fig. 1.** A: Apical four-chamber view. Normal right-sided chambers: the right ventricle is less than one third of the size of the left ventricle. B: Apical four-chamber view. Pulmonary hypertension dilatation and hypertrophy of the right ventricle.

cant degree of LV diastolic dysfunction and eventually - at end stages of PH - of LV systolic dysfunction.<sup>13)</sup> The effect on the LV is the reduction of LV ejection fraction, stroke volume, end-diastolic and end-systolic volume, as well as prolongation of the LV isovolumic relaxation time. The different effects of volume versus pressure-loading of the RV on the LV are best illustrated by the LV eccentricity index. The differences of pressure and volume loading are demonstrated at Table 3.

### QUALITATIVE ASSESSMENT OF THE RIGHT VENTRICLE

#### DILATATION

Normally the RV is 1/3 of the size of the LV in the parasternal long axis view. One of the first changes in the RV in response to the increased preload and afterload is dilatation, which progresses with worsening PH.<sup>7-9)</sup>

#### HYPERTROPHY

In the face of chronically elevated RV afterload, the RV walls become hypertrophied. One of the first anatomical elements to do so is the moderator band, which in normal subjects it is thin and sometimes difficult to see.

#### CONTRACTILITY

In PH, RV impairment is global: this is in contrast to other conditions affecting the RV, such as RV infarction or arrhythmogenic RV cardiomyopathy, where there will be regional wall motion abnormalities.<sup>7,8)</sup>

#### MEASUREMENTS

##### RIGHT ATRIAL PRESSURE

From the subcostal view, measurement of the diameter of the inferior vena cava at end-expiration and during an inspira-

**Table 3.** Difference in measurements between pressure and volume loading

Measurements	Volume loading	Pressure loading	Pressure and volume loading
Dilatation	↑↑	↑	↑↑
Hypertrophy	↑	↑↑	↑↑
Contractility	↓ or ↔	↓↓	↓↓
Tricuspid annular dilatation	↑↑	↑	↑↑
Tricuspid regurgitant jet (volume)	↑↑	↑	↑↑
TAPSE	↔ or ↑	↓	↓ or ↔
LV eccentricity index at end-systole	↔	↑	↑
LV eccentricity index at end-diastole	↑	↔	↑

LV: left ventricle

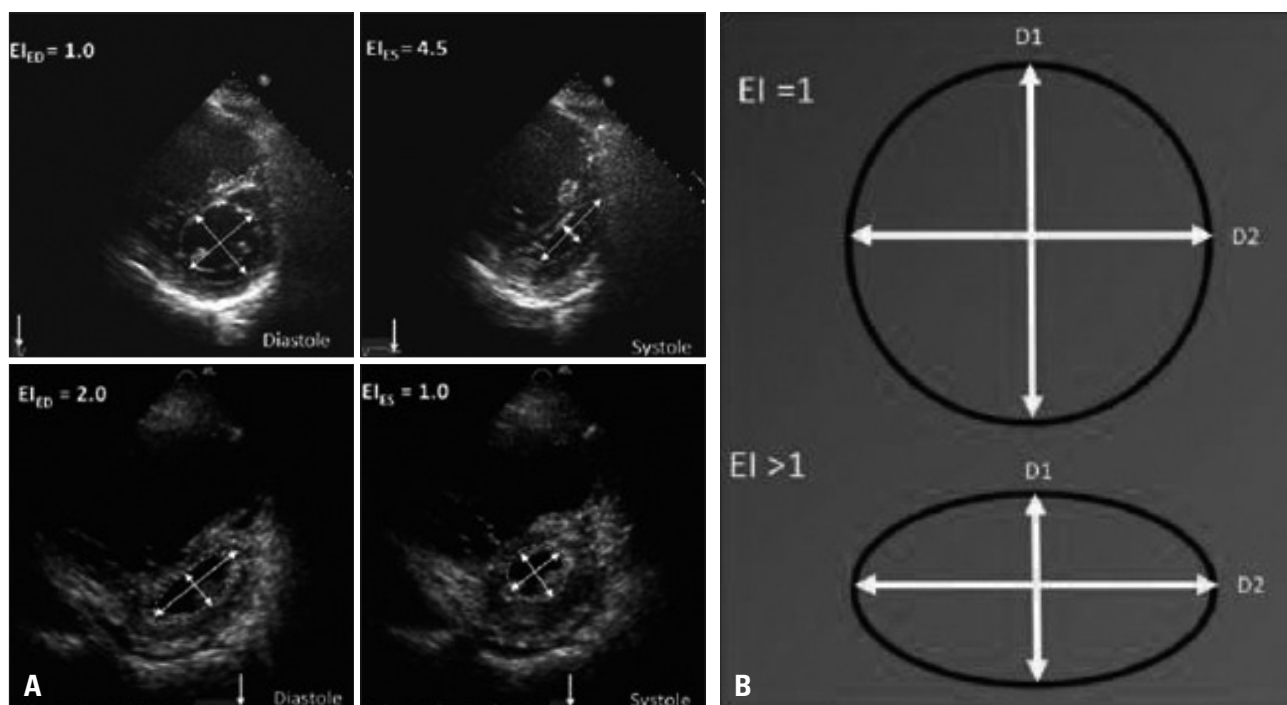


Fig. 2. Examples of the effects of pressure-loading (A) and volume-loading (B) of the right ventricle on the eccentricity index of the left ventricle.

tory manoeuvre provides an estimate of right atrial (RA) pressure. A normal diameter of the inferior vena cava (1.2 to 2.3 cm) and the segment adjacent to the right atrium collapses by at least 50% with respiration, will simply normal right atrial pressure.<sup>3)</sup> Failure for the inferior vena cava to collapse with respiration and/or dilation of the inferior vena cava and hepatic veins is associated with higher right atrial pressures.

**RIGHT VENTRICULAR SYSTOLIC PRESSURE (TRICUSPID REGURGITANT VELOCITY)**

Tricuspid regurgitant velocity is derived from the application of continuous wave Doppler along the tricuspid regurgitant jet, from apical four chamber projections or from the parasternal RV inflow view, if the regurgitant jet is eccentric.<sup>2-5)10)</sup>

The peak velocity reflects the RV to right atrial pressure difference, ΔP, and in the absence of pulmonary stenosis, the RV systolic pressure (RVSP) is assumed to equal pulmonary artery systolic pressure (PASP), and is calculated through the Bernoulli Equation:<sup>4)6)10)11)16)</sup>

$$PASP = RVSP = 4 (V_{TR})^2 + RAP$$

(V<sub>TR</sub>: tricuspid regurgitant velocity, RAP: right atrial pressure)

Note that in cases of severe free-flow tricuspid regurgitation, the Bernoulli equation is not valid.

**PULMONARY ARTERY MEAN AND DIASTOLIC PRESSURE**

As with the tricuspid regurgitant jet, the Bernoulli Equation can be applied to calculate pulmonary arterial end-diastolic pressure (PEDP):<sup>6)10)</sup>

$$PEDP = 4 (V_{ED})^2 + RAP$$

(V<sub>ED</sub>: end-diastolic pulmonary regurgitant velocity)

Mean pulmonary artery pressure, may also be derived from the pulmonary regurgitant velocity:<sup>6)10)</sup>

$$\text{Mean PAP} = 4 (PR V_{BD})^2 + RAP$$

(V<sub>BD</sub>: beginning of diastole pulmonary regurgitant velocity)

**RIGHT VENTRICULAR OUTFLOW TRACT ACCELERATION TIME**

RV outflow tract acceleration time is the time in millisec-

onds from the beginning of the pulmonary ejection until the maximum of the systolic velocity.<sup>11)12)14)15)</sup> It is measured by pulsed-wave Doppler with the sample volume positioned at the centre of the pulmonary artery, ideally at the annulus, in the parasternal short-axis view. In normal people, the acceleration time exceeds 140 ms and it shortens in PH. A value below 105 ms is suggestive of PH.<sup>12)13)</sup> This measurement is particularly important when the peak tricuspid regurgitant jet is not visible.

**MEASUREMENT OF RIGHT ATRIAL VOLUME INDEX**

The measurement of RA volume index is usually performed from the apical four-chamber view or from the subcostal view.<sup>16)18)</sup> Atrial volume is measured at end-systole, where the maximum atrial volume can be obtained.

The single plane area-length method is used and RA volume is measured using the area and the long axis length of the atrium:<sup>3)18)</sup>

$$\text{RA volume index} = (0.85 A^2 / L) / \text{BSA}$$

[A: area of atrium in any view (cm<sup>2</sup>), L: long axis length of atrium (cm), BSA: body surface area]. The normal right atrial volume when indexed for body surface area is 34 mL/m<sup>2</sup> for men and 27 mL/m<sup>2</sup> for women.<sup>18)</sup>

**RIGHT VENTRICULAR FRACTIONAL AREA CHANGE**

RV fractional area change (FAC) is calculated as follows:

$$\text{RV FAC (\%)} = (A_{ED} - A_{ES}) / A_{ED}$$

Where A<sub>ED</sub> is end-diastolic area and A<sub>ES</sub> is end-systolic area, measured from the apical four-chamber view.<sup>3)13)15)23)</sup>

**LEFT VENTRICULAR ECCENTRICITY INDEX**

Eccentricity index is measured by the parasternal short-axis at the level of LV papillary muscles. It is measured as the ratio of the minor axis of the LV parallel to the septum, divided to minor-axis perpendicular to the septum (Fig. 3). The index is measured in end-diastole and end-systole. In a purely pressure-loaded RV, there is flattening of the interventricular sep-

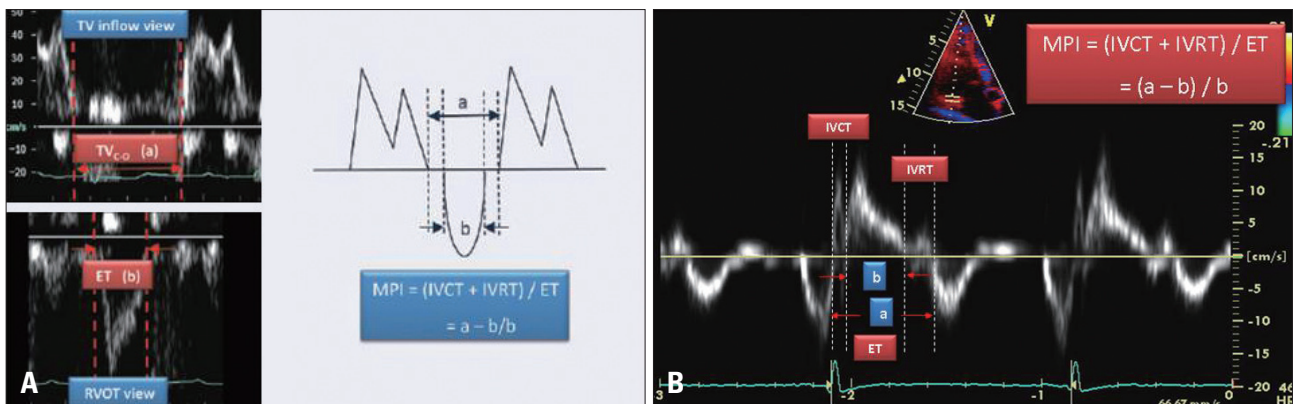


**Fig. 3.** Myocardial performance index. A: Tricuspid inflow from valve opening to closure (TV<sub>Co</sub>) is the sum of isovolumic contraction time (IVCT), ejection time (ET) and isovolumic relaxation time (IVRT). The ejection time - as measured from the short axis RV outflow tract view - is subtracted from TV<sub>Co</sub> and the result is divided by ET to give MPI. B: Measurement of MPI using tissue Doppler imaging.

tum in end-systole, which results in increased end-systolic LV eccentricity index. In pure volume-loading, the eccentricity index will be increased in end-diastole.<sup>615)</sup>

#### TISSUE DOPPLER IMAGING

Two types of tissue Doppler imaging can be applied on the assessment of the RV<sup>1621)22)</sup>

A) Pulsed mode tissue Doppler imaging: Peak velocities and the acceleration and deceleration of structures can be measured. A pulsed-wave Doppler sampling gate of 2-4 mm and a sweep of 100-150 mm/sec are used.

B) Conventional colour Doppler mapping: Measurements are made from the apical four-chamber view, with the patient holding their breath in end-expiration.

#### RV DIASTOLIC DYSFUNCTION

Diastolic dysfunction comprises:

- poor relaxation
- decreased compliance (change in unit volume per unit pressure)

Diastolic function of the RV can be assessed with many parameters, and those useful in PH include:

Isovolumic relaxation time when prolonged, it indicates poor myocardial relaxation. A normal isovolumic relaxation time is  $75 \pm 12$  ms. With abnormal relaxation, the value is usually in excess of 110 ms. However, when restriction is present with high right atrial pressures, isovolumic relaxation time will fall below normal to durations less than 60 ms.<sup>17)22)</sup>

#### Transtricuspid inflow (E wave deceleration)

Deceleration of inflow of the E wave is measured by deceleration time, which shortens with decreasing RV compliance. Deceleration time is complex, as higher RA pressures also shorten it. A normal deceleration time is  $198 \pm 23$  ms; values over 240 ms indicate impaired relaxation, and under 160 ms suggest restriction.<sup>22)23)</sup>

#### MYOCARDIAL PERFORMANCE INDEX OF THE RIGHT VENTRICLE

Myocardial performance index, also known as Tei Index,<sup>21)22)</sup> combines a combination of systolic and diastolic measurements (Fig. 3). The normal range for RV myocardial performance index is 0.28-0.32.<sup>20-22)</sup> It is relatively unaffected by heart rate, loading conditions or the presence and the severity of tricuspid regurgitation. In patients with idiopathic pulmonary arterial hypertension, the index correlates with symptoms and values above 0.88 predict poor survival.

#### S' WAVE VELOCITY

The patient has to be in sinus rhythm and the velocities are indexed to the heart rate. The S' wave velocity is normally greater than 12 cm/sec, and we consider a cut-off value of 11.5 cm/sec, below which RV myocardial function may be

impaired.<sup>20)</sup>

#### TRICUSPID ANNULAR PLANE SYSTOLIC EXCURSION

Tricuspid annular plane systolic excursion is the reflection of the movement the base to apex shortening of the RV in systole (longitudinal function). During ventricular systole, long axis shortening is created by motion of both atrioventricular valve annulae toward the cardiac apex. Because the septal attachment of the tricuspid annulus is relatively fixed, the majority of tricuspid annular motion occurs in its lateral aspect.<sup>19)24-26)</sup>

The measurement of tricuspid annular plane systolic excursion is derived from the apical four chamber view. Special care has to be taken for the whole RV to be included in the view with no dropout in the endocardial outline along the interventricular septum and RV free wall. The width of sector should be limited onto the RV free wall, and the M-mode cursor should be positioned on the lateral portion of the tricuspid annulus, measuring in control sweep mode.

Maximal tricuspid annular plane systolic excursion is defined by the total excursion of the tricuspid annulus from its highest position after atrial ascent to the peak descent during ventricular systole.<sup>24-27)</sup> Earlier studies using two dimensional echocardiography showed that in the normal RV this value exceeds 16 mm. Using M-mode the normal range is higher ( $24.9 \pm 3.5$  mm<sup>25)</sup>;  $25.4 \pm 4.9$  mm<sup>25)26)</sup>) and a value of 20.1 mm has been shown to be a useful cut-off in identifying PH.

#### ADVANCED RIGHT VENTRICULAR IMAGING

##### REAL TIME THREE DIMENSIONAL ECHOCARDIOGRAPHY

Two dimensional echocardiography has been established as the most widely applied imaging tool in clinical cardiology practice. Its application helps in morphological and functional assessment of cardiac chambers and valves. The advancement in technology of echocardiographic machines and its software analysis minimized many difficulties and limitations.<sup>28)29)</sup> However, two dimensional applications still carry some limitations. It requires mental conceptualization of a series of multiple orthogonal planer or tomographic images into an imaginary multidimensional reconstruction for better understanding of complex intracardiac structures and their spatial relation with surroundings. Many of two dimensional formula used for volume quantification and ejection fraction calculation especially for LV are based on geometric assumption that may not true providing varied results in the setting of chamber dilatation or distortion and in the presence of regional wall motion abnormalities.<sup>29)30)</sup>

Three dimensional echocardiography has developed the last 15 years and provides more accurate assessment of ventricular volume, mass and function as well as a more complete view of the valves. The third generation echocardiographic machines with the developed matrix array transducer which consists approximately 3,000 firing elements, have improved the con-

trast resolution and penetration. With this transducer, the entire heart image could be obtained by a pyramidal full-volume acquisition of four cardiac cycles. The development in software made the data off-line analysis faster and easier.

The new modality of real time three dimensional echocardiography (3DE) seems to offer the ability to improve and expand the diagnostic capabilities of cardiac ultrasound.<sup>30-32</sup> The development of 3DE systems circumvents many of the disadvantages of reconstructive methods from two dimensional images. It has been widely applied to the LV with great results and a significant degree of accuracy and reproducibility. Most studies<sup>34-40</sup> that have applied 3D echocardiographic techniques to the RV have involved primarily rotational or free-hand scanning methods: most of these series demonstrated improved accuracy of RV function assessment. Furthermore, several studies<sup>32-40</sup> have compared 3DE with cardiac magnetic resonance imaging (CMR), demonstrating excellent agreement between the two modalities and good intra and inter-observer reproducibility of both.

#### STUDY OF RIGHT VENTRICULAR VOLUMES WITH 3DE

Many 3D data sets require offline processing. The recent development of 3DE has the potential to further improve the ability to assess RV chamber size, volume and function.

In a typical protocol of 3DE, an assessment of ventricular function, valvular morphology and hemodynamic status are included.

#### PROTOCOL

The patient is placed at a left decubitus position, as in two dimensional echocardiography and with the use of a different transducer (central X4 transducer, frequency of 3-4 MHz, volumetric frame rate 16-24 frame/s, imaging depth 6-16 cm, rotation speed 6 Hz and pulse length 2.5 cycles) than the one used for conventional echocardiography, the apical four chambers view is captured. The patient must hold his breath for seconds so that the view to be captured properly.

Using sequential long axis planes of the RV, volumetric data sets were regenerated within offline analysis system (4D analysis, TomTec, Munich, Germany) permitting endocardial contours delineation (Fig. 4). End-diastole phase was defined as the peak of the R wave of the QRS complex and end-systole as the first frame before opening of the tricuspid valve. RV volumes were calculated by manual tracing along the endocardial contours in sequential long axis planes of the ventricle, from ventral to dorsal at 7 mm intervals. Note that when delineating the endocardium, interventricular septum should be included as 1/3 for the normal and 2/3 for the hypertrophied RV. Furthermore, trabeculations should be included in the blood pool. Simpson's rule was employed to calculate values for epicardial and endocardial borders. This allowed calculation of end-diastolic volume, end-systolic volume, stroke volume, ejection fraction and RV mass.

3DE allows quantitative measurements of RV mass without the need to rely on geometric assumptions.<sup>32-34</sup> Using the same full-volume 3D data set of RV volume calculation, it is possible to identify epicardial boundaries of the RV wall. The latter is used to calculate an epicardial cast of the RV at end-diastole. The volume of this cast is then subtracted from the epicardial cast and the volume of RV myocardium is obtained (Fig. 4). By multiplying myocardial volume by the specific density of myocardial muscle (1.05 g/mL), RV mass derives.

Several parameters are estimated such as RV long and short axis in end-diastole, RA long and short axis in end-systole and RA volume, the thickness of lateral free wall through RV short axis (RV wall hypertrophy is defined when the thickness is bigger than 5 mm), tricuspid annular diameter in end-diastole and end-systole and the tethering area between the annulus and the leaflets. In addition, 3DE is useful for the assessment of the tricuspid valve in detail, such as in the case of a tricuspid valve cyst or prolapse.

#### STUDIES COMPARING 3DE AND CMR

Many studies have compared 3DE with CMR on the assessment of the LV and RV.<sup>33-42</sup> However; the groups recruited for the same comparison in RV volumetry were not homogenous. Recently, our group published the comparison of 3D echo and CMR in the homogenous population of 60 pulmonary arterial hypertensive patients.<sup>43</sup> It was proved that 3DE overcomes some of the disadvantages of CMR as it can be routinely used for serial imaging and at the bedside. RV remodeling in PAH patients can be accurately examined by both 3DE and CMR.<sup>44-48</sup> Both are robust and reproducible with CMR being more reproducible for measurements of ejection fraction and RV mass.

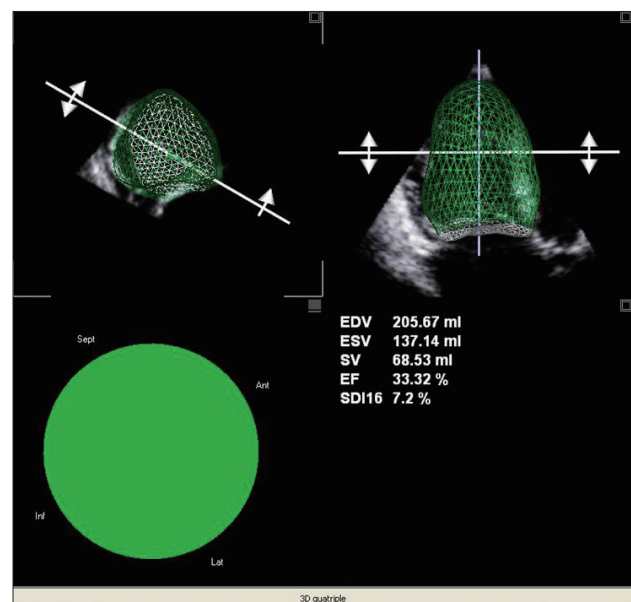


Fig. 4. Calculation of right ventricle volumes and ejection fraction with 3D echocardiography.

**SPECKLE TRACKING - STRAIN**

The speckle pattern is used to track myocardial motion and strain rate is based on the Lagrangian formula which was used to describe systolic deformation.

Speckle tracking has been validated by ultrasonomicrometry in the longitudinal direction and rotation. It has been widely applied to the LV and recently has been introduced for the assessment of the RV in PH.<sup>50</sup> Its advantage is that it is angle-independent and that it can track in two or even three dimensions. Drop-outs and reverberations affect tracking as well as too low or high frame rate. Speckle tracking is frame rate sensitive that is why an adjustment of the frame rate between 50-80 frames per second is the best possible.<sup>49)50)</sup>

**PROTOCOL**

Standard greyscale 2D images are acquired in the 2- and 4-chamber apical views as well as the parasternal short axis views at the level of the papillary muscles. Special care is taken to avoid oblique views from the mid-level short axis images and to obtain images with the most circular geometry possible. All images are recorded with a frame rate of at least 50 fps (50-80 fps) to allow for reliable operation of the software (EchoPAC- GE Healthcare). From an end-systolic single frame, a region of interest is traced on the endocardial cavity interface by a point-and-click approach. Then an automated tracking algorithm follows the endocardium from this single frame throughout the cardiac cycle. All myocardial regions are included. The acoustic markers which are called speckles equally distribute in the region of interest and can follow the entire cardiac cycle. The distance between the speckles is measured as a function of time, and parameters of myocardial deformation are calculated. The RV myocardium is divided into 6 segments and displayed into 6 segmental time-strain curves for radial, circumferential and longitudinal strain (Fig. 5).

**EFFECT OF HEART RATE AND BODY SURFACE AREA**

Most indices of function are unaffected by heart rate, yet

some require correction when heart rate exceeds 100 or drops below 70. These are RV outflow tract acceleration time, myocardial performance index, S' wave velocity and isovolumic relaxation time. In order to index to heart rate, the measurement should be multiplied by 75/heart rate, eg:

$$\text{RV outflow tract acceleration time (indexed to heart rate)} = \text{RV outflow tract acceleration time} \times 75/\text{heart rate}$$

When indexing measurements for body surface area (BSA), they should be divided by the BSA (Dupois & Dupois), where:

$$\text{BSA} = 0.007184 \times \text{weight (kg)} + 0.425 \times \text{height (cm)} - 0.725$$

For the normal man, BSA is 1.9 m<sup>2</sup> and for the normal woman, BSA is 1.6 m<sup>2</sup>.

**STROKE VOLUME, CARDIAC OUTPUT AND PULMONARY VASCULAR RESISTANCE**

Echocardiography uses the combination of two dimensional and pulsed-wave Doppler imaging to measure cardiac output.<sup>3)49)</sup> Stroke volume can be derived from the product of the velocity time integral of the Doppler profile and the cross-sectional area of the LV outflow tract. Cardiac output is the product of stroke volume and heart rate.

$$\text{Stroke volume} = \text{velocity time integral (LV outflow tract)} \times \text{cross-sectional area (LV outflow tract)}$$

$$\text{Cardiac output} = \text{stroke volume} \times \text{heart rate}$$

Similarly, RV stroke volume and cardiac output can be measured from the proximal RV outflow tract, just within the pulmonary valve from the parasternal short-axis view.

In order to calculate pulmonary vascular resistance, continuous-wave Doppler is used to determine the peak tricuspid regurgitant velocity as described above: the highest velocity is used. In patients with atrial fibrillation, the average of five measurements should be taken.

$$\text{Pulmonary vascular resistance (Wood units)} = 10 \cdot (\text{peak tricuspid regurgitant velocity} / \text{velocity time integral}_{\text{RVoutflow tract}}) + 0.16$$

This measurement has been shown to correlate well with pulmonary vascular resistance measured at cardiac catheterisation

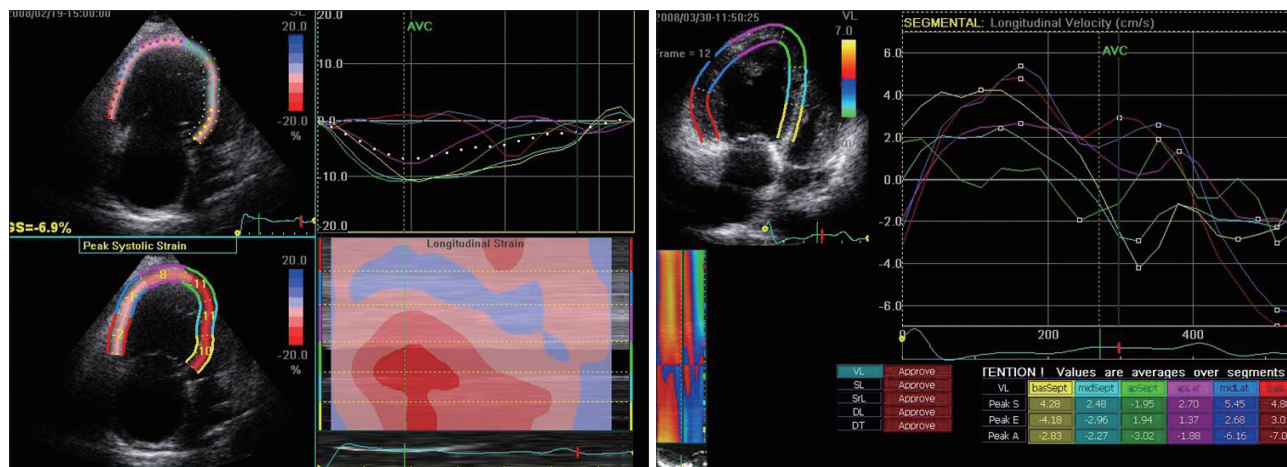


Fig. 5. Right ventricle speckle tracking.



over a range of right and left atrial pressures. A value of peak tricuspid regurgitant velocity/velocity time integral  $_{RVoutflow tract}$  less than 0.2 has 94% sensitivity for a pulmonary vascular resistance of less than 2 Wood Units at catheterisation.<sup>51)</sup> As the definition of pulmonary arterial hypertension includes a pulmonary vascular resistance greater than 3 Wood Units, a value of peak tricuspid regurgitant velocity/velocity time integral  $_{RVoutflow tract}$  less than 0.2 will exclude most cases of pulmonary arterial hypertension. While measures of stroke volume, cardiac output and pulmonary vascular resistance are readily measurable at echocardiography and correlate with right and left heart function and the underlying pulmonary vascular resistance, these measurements are not considered core to the protocol and are thus not mandatory measurements. The value of serial measurements in the follow-up of PH has not been validated.

### OUTCOMES IN PULMONARY HYPERTENSION

The primary abnormality in PH is increased afterload on the RV due to elevated pulmonary vascular resistance caused by remodelling of the resistance pulmonary arteries. It is possible that the RV itself is predisposed to abnormal remodelling due to the same genetic abnormalities underlying vascular remodelling, but this is highly speculative. Nonetheless, it is clear from many studies that it is cardiac function which determines prognosis and exercise capacity. In particular, it is worth noting that pulmonary arterial pressure by itself does not correlate at all well with exercise capacity or prognosis. This is made abundantly obvious from the fact that pulmonary arterial pressure will fall with advancing RV failure. As RV failure progresses, cardiac output falls and right atrial pressure rises. Values from cardiac catheterisation associated with poor prognosis are:<sup>52-54)</sup>

- Cardiac index < 2.1 L/min/m<sup>2</sup>
- Right atrial pressure > 10 mmHg
- Mixed venous oxygen saturation < 63%

(low values indicate increased oxygen extraction due to lower cardiac output)

In line with these measurements, echocardiographic follow-up studies have shown increased right atrial size to be associated with poor prognosis. Persistently high right atrial pressure may lead to the development of a pericardial effusion, which is a powerful predictor of mortality.

Other echocardiographic features that have been shown to correlate with survival<sup>51-53)</sup> include markers of myocardial function such as myocardial performance index, RV fractional area change and tricuspid annular plane systolic excursion. A cut-off value of greater than 0.88 for myocardial performance index and less than 15 mm for tricuspid annular plane systolic excursion have been particularly associated with poor prognosis. Increases in LV eccentricity index at end-diastole have also been shown in several studies to be associated with worse outcomes, indicating the adverse impact of LV compression. Pa-

tients with values above 1.7 have a significantly higher risk of dying. While it may be important to use cut-off values from echocardiography to risk-stratify patients, there are many other powerful clinical indicators of severity, such as functional class, hemodynamics and exercise capacity. Nonetheless, there are problems with using these measures in following the clinical course of patients or response to therapy. Hemodynamics can only be obtained by invasive means; functional class is a crude assessment for only small to moderate change; and exercise capacity can be influenced by many other factors.

### SUMMARY

This review paper demonstrated the best assessment of the RV with current echocardiography and the evolution of new imaging techniques such as real time 3DE and speckle tracking. Echocardiography can assess sufficiently RV structure and function and also suggest prognosis in PH patients.

#### • Acknowledgements

We would like to thank the Consultants of National Pulmonary Hypertension Service, Dr. J Simon R Gibbs and Dr. Luke SGE Howard for their help and support.

### REFERENCES

1. Foale R, Nihoyannopoulos P, McKenna W, Kleinebenne A, Nadazdin A, Rowland E, Smith G. *Echocardiographic measurement of the normal adult right ventricle*. *Br Heart J* 1986;56:33-44.
2. Vahanian A, Baumgartner H, Bax J, Butchart E, Dion R, Filippatos G, Flachskampf F, Hall R, Jung B, Kasprzak J, Nataf P, Tornos P, Torracca L, Wenink A. *Guidelines on the management of valvular heart disease: The Task Force on the Management of Valvular Heart Disease of the European Society of Cardiology*. *Eur Heart J* 2007;28:230-68.
3. Lang RM, Bierig M, Devereux RB, Flachskampf FA, Foster E, Pellikka PA, Picard MH, Roman MJ, Seward J, Shanewise JS, Solomon SD, Spencer KT, Sutton MS, Stewart WJ. *Recommendations for chamber quantification: a report from the American Society of Echocardiography's Guidelines and Standards Committee and the Chamber Quantification Writing Group, developed in conjunction with the European Association of Echocardiography, a branch of the European Society of Cardiology*. *J Am Soc Echocardiogr* 2005;18:1440-63.
4. Kaul S, Tei C, Hopkins JM, Shah PM. *Assessment of right ventricular function using two-dimensional echocardiography*. *Am Heart J* 1984;107:526-31.
5. Santamore WP, Dell'Italia LJ. *Ventricular interdependence: significant left ventricular contributions to right ventricular systolic function*. *Prog Cardiovasc Dis* 1998;40:289-308.
6. López-Candales A, Dohi K, Rajagopalan N, Edelman K, Gulyasy B, Bazaz R. *Defining normal variables of right ventricular size and function in pulmonary hypertension: an echocardiographic study*. *Postgrad Med J* 2008;84:40-5.
7. Haddad F, Hunt SA, Rosenthal DN, Murphy DJ. *Right ventricular function in cardiovascular disease, part I: anatomy, physiology, aging, and functional assessment of the right ventricle*. *Circulation* 2008;117:1436-48.
8. Haddad F, Doyle R, Murphy DJ, Hunt SA. *Right ventricular function in cardiovascular disease, part II: pathophysiology, clinical importance, and management of right ventricular failure*. *Circulation* 2008;117:1717-31.
9. Schnittger I, Gordon EP, Fitzgerald PJ, Popp RL. *Standardized intracardiac measurements of two-dimensional echocardiography*. *J Am Coll Cardiol* 1983;2:934-8.

10. Zoghbi WA, Enriquez-Sarano M, Foster E, Grayburn PA, Kraft CD, Levine RA, Nihoyannopoulos P, Otto CM, Quinones MA, Rakowski H, Stewart WJ, Waggoner A, Weissman NJ. *Recommendations for evaluation of the severity of native valvular regurgitation with two-dimensional and Doppler echocardiography.* *J Am Soc Echocardiogr* 2003;16:777-802.
11. Fisher MR, Forfia PR, Chamera E, Houston-Harris T, Champion HC, Girgis RE, Corretti MC, Hassoun PM. *Accuracy of Doppler echocardiography in the hemodynamic assessment of pulmonary hypertension.* *Am J Respir Crit Care Med* 2009;179:615-21.
12. Kitabatake A, Inoue M, Asao M, Masuyama T, Tanouchi J, Morita T, Mishima M, Uematsu M, Shimazu T, Hori M, Abe H. *Noninvasive evaluation of pulmonary hypertension by a pulsed Doppler technique.* *Circulation* 1983;68:302-9.
13. Stein PD, Sabbah HN, Anbe DT, Marzilli M. *Performance of the failing and nonfailing right ventricle of patients with pulmonary hypertension.* *Am J Cardiol* 1979;44:1050-5.
14. Yoshida K, Yoshikawa J, Shakudo M, Akasaka T, Jyo Y, Takao S, Shiratori K, Koizumi K, Okumachi F, Kato H. *Color Doppler evaluation of valvular regurgitation in normal subjects.* *Circulation* 1988;78:840-7.
15. Schnittger I, Gordon EP, Fitzgerald PJ, Popp RL. *Standardized intracardiac measurements of two-dimensional echocardiography.* *J Am Coll Cardiol* 1983;2:934-8.
16. Olson JM, Samad BA, Alam M. *Prognostic value of pulse-wave tissue Doppler parameters in patients with systolic heart failure.* *Am J Cardiol* 2008;102:722-5.
17. Abbas A, Lester S, Moreno FC, Srivathsan K, Fortuin D, Appleton C. *Noninvasive assessment of right atrial pressure using Doppler tissue imaging.* *J Am Soc Echocardiogr* 2004;17:1155-60.
18. Wang Y, Gutman JM, Heilbron D, Wahr D, Schiller NB. *Atrial volume in a normal adult population by two-dimensional echocardiography.* *Chest* 1984;86:595-601.
19. Forfia PR, Fisher MR, Mathai SC, Houston-Harris T, Hemnes AR, Borlaug BA, Chamera E, Corretti MC, Champion HC, Abraham TP, Girgis RE, Hassoun PM. *Tricuspid annular displacement predicts survival in pulmonary hypertension.* *Am J Respir Crit Care Med* 2006;174:1034-41.
20. Dujardin KS, Tei C, Yeo TC, Hodge DO, Rossi A, Seward JB. *Prognostic value of a Doppler index combining systolic and diastolic performance in idiopathic-dilated cardiomyopathy.* *Am J Cardiol* 1998;82:1071-6.
21. Tei C, Dujardin KS, Hodge DO, Bailey KR, McGoon MD, Tajik AJ, Seward SB. *Doppler echocardiographic index for assessment of global right ventricular function.* *J Am Soc Echocardiogr* 1996;9:838-47.
22. Yeo TC, Dujardin KS, Tei C, Mahoney DW, McGoon MD, Seward JB. *Value of a Doppler-derived index combining systolic and diastolic time intervals in predicting outcome in primary pulmonary hypertension.* *Am J Cardiol* 1998;81:1157-61.
23. Hatle L, Angelsen B. *Doppler ultrasound in cardiology: physical principles and clinical applications.* 2nd ed. Philadelphia: Lea & Febiger; 1985:93.
24. Meluzín J, Spinarová L, Bakala J, Toman J, Krejčí J, Hude P, Kára T, Soucek M. *Pulsed Doppler tissue imaging of the velocity of tricuspid annular systolic motion; a new, rapid, and non-invasive method of evaluating right ventricular systolic function.* *Eur Heart J* 2001;22:340-8.
25. Lee CY, Chang SM, Hsiao SH, Tseng JC, Lin SK, Liu CP. *Right heart function and scleroderma: insights from tricuspid annular plane systolic excursion.* *Echocardiography* 2007;24:118-25.
26. Hammarström E, Wranne B, Pinto FJ, Puryear J, Popp RL. *Tricuspid annular motion.* *J Am Soc Echocardiogr* 1991;4:131-9.
27. Nath J, Foster E, Heidenreich PA. *Impact of tricuspid regurgitation on long-term survival.* *J Am Coll Cardiol* 2004;43:405-9.
28. Lang RM, Mor-Avi V, Sugeng L, Nieman PS, Sahn DJ. *Three-dimensional echocardiography: the benefits of the additional dimension.* *J Am Coll Cardiol* 2006;48:2053-69.
29. Tandri H, Daya SK, Nasir K, Bomma C, Lima JA, Calkins H, Bluemke DA. *Normal reference values for the adult right ventricle by magnetic resonance imaging.* *Am J Cardiol* 2006;98:1660-4.
30. Mannaerts HF, van der Heide JA, Kamp O, Stoel MG, Twisk J, Visser CA. *Early identification of left ventricular remodelling after myocardial infarction, assessed by transthoracic 3D echocardiography.* *Eur Heart J* 2004;25:680-7.
31. King DL, Gopal AS, Keller AM, Sapin PM, Schröder KM. *Three-dimensional echocardiography. Advances for measurement of ventricular volume and mass.* *Hypertension* 1994;23:1172-9.
32. van den Bosch AE, Robbers-Visser D, Krenning BJ, McGhie JS, Helbing WA, Meijboom FJ, Roos-Hesselink JW. *Comparison of real-time three-dimensional echocardiography to magnetic resonance imaging for assessment of left ventricular mass.* *Am J Cardiol* 2006;97:113-7.
33. Kjaergaard J, Petersen CL, Kjaer A, Schaadt BK, Oh JK, Hassager C. *Evaluation of right ventricular volume and function by 2D and 3D echocardiography compared to MRI.* *Eur J Echocardiogr* 2006;7:430-8.
34. Fujimoto S, Mizuno R, Nakagawa Y, Dohi K, Nakano H. *Estimation of the right ventricular volume and ejection fraction by transthoracic three-dimensional echocardiography. A validation study using magnetic resonance imaging.* *Int J Card Imaging* 1998;14:385-90.
35. Katz J, Whang J, Boxt LM, Barst RJ. *Estimation of right ventricular mass in normal subjects and in patients with primary pulmonary hypertension by nuclear magnetic resonance imaging.* *J Am Coll Cardiol* 1993;21:1475-81.
36. Grothues F, Moon JC, Bellenger NG, Smith GS, Klein HU, Pennell DJ. *Interstudy reproducibility of right ventricular volumes, function, and mass with cardiovascular magnetic resonance.* *Am Heart J* 2004;147:218-23.
37. Helbing WA, Rebergen SA, Maliepaard C, Hansen B, Ottenkamp J, Reiber JH, de Roos A. *Quantification of right ventricular function with magnetic resonance imaging in children with normal hearts and with congenital heart disease.* *Am Heart J* 1995;130:828-37.
38. Alfakih K, Reid S, Jones T, Sivananthan M. *Assessment of ventricular function and mass by cardiac magnetic resonance imaging.* *Eur Radiol* 2004;14:1813-22.
39. Lorenz CH, Walker ES, Morgan VL, Klein SS, Graham TP Jr. *Normal human right and left ventricular mass, systolic function, and gender differences by cine magnetic resonance imaging.* *J Cardiovasc Magn Reson* 1999;1:7-21.
40. Pattynama PM, Lamb HJ, Van der Velde EA, Van der Geest RJ, Van der Wall EE, De Roos A. *Reproducibility of MRI-derived measurements of right ventricular volumes and myocardial mass.* *Magn Reson Imaging* 1995;13:53-63.
41. Angelini ED, Homma S, Pearson G, Holmes JW, Laine AF. *Segmentation of real-time three-dimensional ultrasound for quantification of ventricular function: a clinical study on right and left ventricles.* *Ultrasound Med Biol* 2005;31:1143-58.
42. van Wolferen SA, Marcus JT, Boonstra A, Marques KM, Bronzwaer JG, Spreeuwenberg MD, Postmus PE, Vonk-Noordegraaf A. *Prognostic value of right ventricular mass, volume, and function in idiopathic pulmonary arterial hypertension.* *Eur Heart J* 2007;28:1250-7.
43. Grapsa J, O'Regan DP, Pavlopoulos H, Durighel G, Dawson D, Nihoyannopoulos P. *Right ventricular remodelling in pulmonary arterial hypertension with three-dimensional echocardiography: comparison with cardiac magnetic resonance imaging.* *Eur J Echocardiogr* 2010;11:64-73.
44. Nesser HJ, Tkalec W, Patel AR, Masani ND, Niel J, Markt B, Pandian NG. *Quantitation of right ventricular volumes and ejection frac-*

- tion by three-dimensional echocardiography in patients: comparison with magnetic resonance imaging and radionuclide ventriculography. *Echocardiography* 2006;23:666-80.
45. Niemann PS, Pinho L, Balbach T, Galuschky C, Blankenhagen M, Silberbach M, Broberg C, Jerosch-Herold M, Sahn DJ. Anatomically oriented right ventricular volume measurements with dynamic three-dimensional echocardiography validated by 3-Tesla magnetic resonance imaging. *J Am Coll Cardiol* 2007;50:1668-76.
  46. Gopal AS, Chukwu EO, Iwuchukwu CJ, Katz AS, Toole RS, Schapiro W, Reichel N. Normal values of right ventricular size and function by real-time 3-dimensional echocardiography: comparison with cardiac magnetic resonance imaging. *J Am Soc Echocardiogr* 2007;20:445-55.
  47. Lu X, Nadvoretzkiy V, Bu L, Stolpen A, Ayres N, Pignatelli RH, Kovalchin JP, Grenier M, Klas B, Ge S. Accuracy and reproducibility of real-time three-dimensional echocardiography for assessment of right ventricular volumes and ejection fraction in children. *J Am Soc Echocardiogr* 2008;21:84-9.
  48. Rademakers FE. 3D echocardiography: is CMR better? *Eur J Echocardiogr* 2006;7:339-40.
  49. Badano LP, Ghingina C, Easaw J, Muraru D, Grillo MT, Lancellotti P, Pinamonti B, Coghlan G, Marra MP, Popescu BA, De Vita S. Right ventricle in pulmonary arterial hypertension: haemodynamics, structural changes, imaging, and proposal of a study protocol aimed to assess remodelling and treatment effects. *Eur J Echocardiogr* 2010;11:27-37.
  50. Padeletti M, Cameli M, Lisi M, Zacà V, Tsioulpas C, Bernazzali S, Maccherini M, Mondillo S. Right atrial speckle tracking analysis as a novel noninvasive method for pulmonary hemodynamics assessment in patients with chronic systolic heart failure. *Echocardiography* 2011;28:658-64.
  51. Abbas AE, Fortuin FD, Schiller NB, Appleton CP, Moreno CA, Lester SJ. A simple method for noninvasive estimation of pulmonary vascular resistance. *J Am Coll Cardiol* 2003;41:1021-7.
  52. British Cardiac Society Guidelines and Medical Practice Committee, and approved by the British Thoracic Society and the British Society of Rheumatology. Recommendations on the management of pulmonary hypertension in clinical practice. *Heart* 2001;86 Suppl 1:11-13.
  53. Raymond RJ, Hinderliter AL, Willis PW, Ralph D, Caldwell EJ, Williams W, Ettinger NA, Hill NS, Summer WR, de Boisblanc B, Schwartz T, Koch G, Clayton LM, Jöbsis MM, Crow JW, Long W. Echocardiographic predictors of adverse outcomes in primary pulmonary hypertension. *J Am Coll Cardiol* 2002;39:1214-9.
  54. Ghio S, Klersy C, Magrini G, D'Armini AM, Scelsi L, Raineri C, Pasotti M, Serio A, Campana C, Viganò M. Prognostic relevance of the echocardiographic assessment of right ventricular function in patients with idiopathic pulmonary arterial hypertension. *Int J Cardiol* 2010;140:272-8.